# PURE IN-PLANE SHEAR BEHAVIOUR OF A STEEL-CONCRETE-STEEL SANDWICH STRUCTURE DEPENDING ON THE REINFORCEMENT RATIO

*Roman Kubát, **

Katedra betonových a zděných konstrukcí, Fakulta stavební,
České vysoké učení technické v Praze, Thákurova 7/2077, 166 29 Praha 6, Česká republika.
roman.kubat@fsv.cvut.cz

**ABSTRAKT**

Tento článek se zabývá způsoby porušení ocelobetonového sendviče při čistě smykovém zatížení v rovině konstrukce. Úvodem je představena problematika závislosti způsobu porušení na poměru vyztužení ocelobetonového sendviče. Prozatímní experimentální výzkum společně s vyvinutými modely naznačují, že při zvyšujícím se poměru vyztužení se snižuje duktilita konstrukce s možným drcením tlačené betonové diagonály před dosažením meze kluzu oceli v tahu. Pro seznámení čtenáře s chováním ocelobetonového sendviče v rovinném smyku je uveden stručný popis analytického modelu. Dále je popsán japonský experimentální program, který zkoumal chování panelů se stupněm vyztužení 2,3%, 3,2% a 4,5%. Výsledky zkoušek poslouží ke kalibraci nelineárního numerického modelu a následné extrapolaci experimentálních výsledků pro vyšší poměry vyztužení. V závěru je představena dosavadní vlastní práce autora na modelování daného problému společně s výhledy na další úpravy.

**KLÍČOVÁ SLOVA**

Ocelobetonový sendvič • Rovinný smyk • Poměr vyztužení • Způsob porušení • Smyková odezva

**ABSTRACT**

This paper deals with failure modes of a steel-concrete-steel sandwich loaded by pure in-plane shear. Current research together with the developed models imply that increase of reinforcement ratio leads to decrease of ductility and possibly to change a failure mode from yielding of steel in tension to crushing of concrete in compression which results in brittle failure. In order to give a reader basic information about in-plane shear behaviour of a steel-concrete-steel sandwich, an analytical model is introduced. Japanese experimental program that researched a behaviour of SCS panels with reinforcement ratio 2.3%, 3.2% and 4.5% is also shown. Results of the tests serve for calibration of a numerical nonlinear model. In the end, an achieved work on shear behaviour modelling, that have been done so far, is introduced.

**KEYWORDS**

Steel-concrete-steel sandwich • In-plane shear • Reinforcement ratio • Failure mode • Force-shear response

## 1. INTRODUCTION

A steel-concrete-steel sandwich (SCS) structure consists of two external steel plates, which are anchored to infill concrete. The composite action is mostly provided by a combination of headed studs and tie bars.

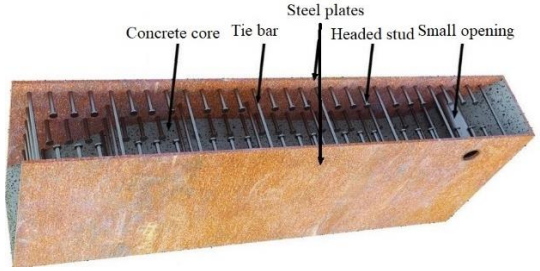


Figure 1 SCS structure

The SCS works quite like classical reinforced concrete (RC). The steel plates carry the tension forces and the concrete increases compression strength and stability. However, the construction solution of SCS can provide much more resistance than classic RC, and that is the reason why the area of use of SCS is principally in extremely loaded structures like protective structures, offshore structures, oil storage containers, ice-resistant structures, and containments of nuclear reactors.

On the other hand, a lack of experience might cause design problems. Currently, there are only few findable codes, which provide the design methods for SCS. The only one available is ANSI/AISC N690-18 (American Institute of Steel Construction, 2018). The code summarizes knowledge acquired from experimental research. Unfortunately, it has its limits, which mostly come from the already mentioned lack of experience. One of the most significant is the steel-concrete ratio limitation, which is formulated by the values from 0,015 to 0,05. The use of a very low ratio under 0,015 is generally not recommended to provide sufficient stiffness for concrete placement and transport operations. The higher limit should

* Školitel: doc. Ing. Petr Bílý, Ph.D.

provide the ductility of a structure. The code states that a very high reinforcement ratio might cause the change of the in-plane shear failure mode from faceplate yielding to concrete failure in compression.

Ozaki et al. (2004) and Varma et al. (2011) have been dealing with in-plane shear behaviour. Ozaki et al., they performed several tests on SCS specimens with the reinforcement ratio from 0.023 to 0.045. Varma et al. developed a mechanics-based model, which correlate well with Ozaki´s experimental results. The analytical model is able to extrapolate the experimental results. The extrapolation confirms the failure mode change statement. Unfortunately, the analytical model is unable to consider nonlinear behaviour of concrete including concrete cracking. Since that, the aim of this study is to proof the statement by a numerical nonlinear model.

## 2. MECHANICS-BASED MODEL FOR IN-PLANE BEHAVIOUR

The analytical model is based on the several following simplifying assumptions:

- Perfect composite action of the steel plates and the concrete core.
- Zero tension contribution of the cracked concrete.
- Isotropic elastic plane-stress behaviour for the steel plates.
- Isotropic elastic behaviour for the concrete core before cracking.
- Orthotropic elastic behaviour of the concrete core after cracking with zero stiffness in the principal tensile direction perpendicular to cracking, and 70% of the elastic stiffness for the principal compressive direction parallel to cracking.

Using the Hooke´s law and the above stated assumptions, we get the following equilibrium:

$$\begin{Bmatrix}\varepsilon_x\\ \varepsilon_y\\ \gamma_{xy}\end{Bmatrix}=\left[A_s\cdot[K_s]+A_c\cdot[K_c]\right]^{-1}\begin{Bmatrix}S_x\\ S_y\\ S_{xy}\end{Bmatrix} \quad (1)$$

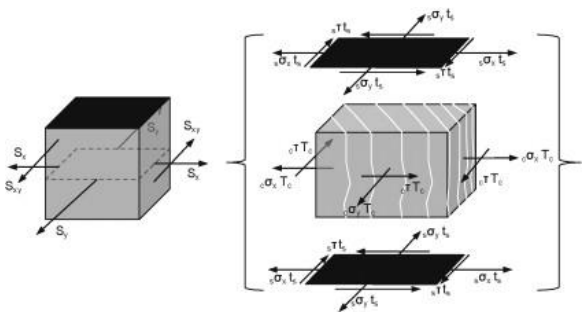

Figure 2 Force equilibrium of composite section (Varma et al., 2011)

Where $A_s$ is the section area of both steel plates, $A_c$ is the section area of concrete core, $K_s$ is the stiffness matrix of steel plates, $K_c$ is the stiffness matrix of concrete core, and $S$ are membrane in-plane forces.

$$[K_s]=\frac{E_s}{1-\upsilon^2}\begin{pmatrix}1 & \upsilon & 0\\ \upsilon & 1 & 0\\ 0 & 0 & \frac{1-\upsilon}{2}\end{pmatrix} \quad (2)$$

$$[K_c]=\frac{E_{cm}}{1-\upsilon^2}\begin{pmatrix}1 & \upsilon & 0\\ \upsilon & 1 & 0\\ 0 & 0 & \frac{1-\upsilon}{2}\end{pmatrix} \quad (3)$$

The stiffness matrixes stated above correspond to isotropic elastic plane-stress behaviour of both materials before concrete cracking. The post-cracking orthotropic behaviour of the concrete core is considered by the following modification of the stiffness matrix:

$$[K_c]=[T]_\sigma^{-1}\begin{pmatrix}a\cdot 0.7\cdot E_{cm} & 0 & 0\\ 0 & b\cdot 0.7\cdot E_{cm} & 0\\ 0 & 0 & 0\end{pmatrix}[T]_\varepsilon \quad (4)$$

Where $T$ is the transformation matrix, $E_{cm}$ is the elastic modulus of concrete core, $E_s$ is the elastic modulus of steel plates, and $v$ is the Poisson´s coeficient. Coefficients $a$ and $b$ consider the concrete cracking. If the principal stress is tensile, the value of the coefficient is 0. For example, both $a$ and $b$ are equal to 1 for biaxial compression. For biaxial tension, both are equal to 0 and for in-plane shear, one is equal to 1 and the other one is equal to 0, depending on the principal stress character in the corresponding direction.

$$[T]_\sigma=\frac{1}{2}\begin{bmatrix}1+\cos(2\theta) & 1-\cos(2\theta) & 2\sin(2\theta)\\ 1-\cos(2\theta) & 1+\cos(2\theta) & -2\sin(2\theta)\\ -\sin(2\theta) & \sin(2\theta) & 2\cos(2\theta)\end{bmatrix} \quad (5)$$

$$[T]_\varepsilon=\frac{1}{2}\begin{bmatrix}1+\cos(2\theta) & 1-\cos(2\theta) & \sin(2\theta)\\ 1-\cos(2\theta) & 1+\cos(2\theta) & -\sin(2\theta)\\ -2\sin(2\theta) & 2\sin(2\theta) & 2\cos(2\theta)\end{bmatrix} \quad (6)$$

By substituting $\theta = 45°$, $a = 1$, $b = 0$ or $\theta = 135°$, $a = 0$ and $b = 1$, which corresponds to pure in-plane shear, the stiffness matrix of the concrete core become:

$$[K_c]=\frac{0.7\cdot E_{cm}}{4}\begin{pmatrix}1 & 1 & -1\\ 1 & 1 & -1\\ -1 & -1 & 1\end{pmatrix} \quad (7)$$

Thus, the modified equilibrium for pure in-plane shear looks as follow:

$$\begin{Bmatrix}0\\ 0\\ S_{xy}\end{Bmatrix}=\left[\frac{E_s\cdot t_s\cdot 2}{1-\upsilon^2}\begin{pmatrix}1 & \upsilon & 0\\ \upsilon & 1 & 0\\ 0 & 0 & \frac{1-\upsilon}{2}\end{pmatrix}+\frac{0.7\cdot E_{cm}\cdot t_c}{4}\begin{pmatrix}1 & 1 & -1\\ 1 & 1 & -1\\ -1 & -1 & 1\end{pmatrix}\right]\begin{Bmatrix}\varepsilon_x\\ \varepsilon_y\\ \gamma_{xy}\end{Bmatrix} \quad (8)$$

### 2.1. Pure in-plane shear

Using the equilibrium (8), it is possible to create a tri-linear force-shear diagram to generalize the in-plane shear response of the SCS.

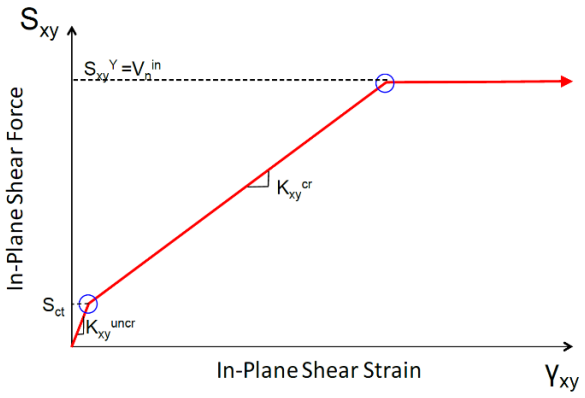

Figure 3: Tri-linear force-shear diagram (Ozaki et al., 2004)

The first part of the curve represents SCS in-plane shear behaviour before concrete cracks in parallel to the compression principal stress. The inclination corresponds to the stiffness of a SCS section with an uncracked concrete.

$$K_{xy}^{uncr} = G_s \cdot A_s + G_c \cdot A_c \quad (9)$$

According to ANSI/AISC N690-18 (American Institute of Steel Construction, 2018), concrete cracking occurs when:

$$S_{xy} = S_{st} = \left( \frac{10.5 \cdot \sqrt{f_c}}{G_c} - \varepsilon_{sh} \right) (G_s \cdot A_s + G_c \cdot A_c) \quad (10)$$

Where $f_c$ is the compressive strength of the concrete core, $\varepsilon_{sh}$ is the shrinkage strain, $G_s$ is the shear modulus of elasticity of steel, and $G_c$ is the shear modulus of elasticity of concrete.

The second part of the curve represents SCS in-plane shear behaviour after concrete cracking occurs. The stiffness of this part is given by:

$$K_{xy}^{cr} = K_s + K_c^{cr} \quad (11)$$

$$K_s = G_s \cdot A_s \quad (12)$$

$$K_c^{cr} = \frac{1}{\frac{4}{0.7 \cdot E_{cm} \cdot A_c} + \frac{2(1-\upsilon)}{E_s \cdot A_s}} \quad (13)$$

Where $K_s$ is the contribution of the steel plates to the in-plane shear stiffness and $K_c^{cr}$ is the contribution of the cracked orthotropic concrete to the in-plane shear stiffness.

The ultimate shear strength is reached when von Mises yielding of the steel plates occurs.

$$S_{xy}^{y} = \frac{K_s + K_c^{cr}}{\sqrt{3 \cdot K_s^2 + K_c^{cr2}}} \cdot A_s \cdot F_y \quad (14)$$

Where $F_y$ is the yield stress of the steel plates.

The last part of the curve describes plastic behaviour after the steel plates reach von Mises yielding. It needs to be mentioned that this model does not consider the possibility of a compressive failure of the concrete core. According to that, the principal compressive stress in concrete must be controlled.

$$\begin{Bmatrix} \sigma_{p,c1} \\ 0 \\ 0 \end{Bmatrix} = \begin{pmatrix} 0,7 \cdot E_{cm} & 0 & 0 \\ 0 & 0 & 0 \\ 0 & 0 & 0 \end{pmatrix} [T]_\varepsilon \begin{Bmatrix} \varepsilon_x \\ \varepsilon_y \\ \gamma_{xy} \end{Bmatrix} \leq f_c \quad (15)$$

The code solves the problem, that a compressive failure of concrete is not considered by the model, by a limitation of the reinforcement ratio to max. 0.05 as mentioned in the introduction.

## 3. JAPANESE EXPERIMENTAL PROGRAM

### 3.1. Parameters of the experiment

The experimental program by Ozaki et al. (2004) includes nine SCS panels. All the panels were 1200 x 1200 mm in in-plane dimensions and 200 mm thick. The composite action was provided by headed stud bolts, which were spaced at intervals of a ratio in which the span (B) of the stud bolts was divided by the thickness (t) of the surface steel plate, B/t = 30. This ratio should avoid the buckling of the steel plates according to Sasaki et al., (1995). In addition, a partitioning web was inserted into two specimens (see Figure 4). The specimens differed also by the thickness of the steel plates (2.3 mm, 3.2 mm, 4.5 mm).

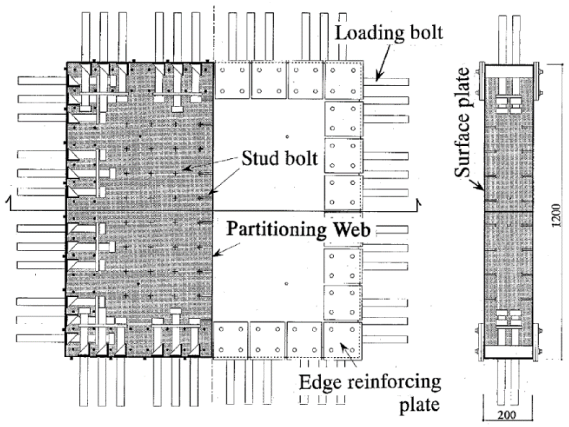


Figure 4: Specimen S3-00PS (Ozaki et al., 2004)

Three specimens were subjected to cyclic pure in-plane shear. The others were loaded by cyclic in-plane shear in a combination with axial forces. Table 1. summarizes all parameters of the specimens.

| Specimens | Surface steel plate ($t$) (mm) | Headed stud bolt | | | Nodal force (MPa) | Partitioning web |
|---|---|---|---|---|---|---|
| | | Pitch in welding ($B$) (mm) | Diameters (mm) | $B/t$ | | |
| S2-00NN | 2.3 | 70 | 4 | 30 | 0.0 | |
| S2-15NN | | | | | 1.47 | |
| S2-30NN | | | | | 2.94 | |
| S3-00NN | 3.2 | 100 | 5 | 31 | 0.0 | |
| S3-15NN | | | | | 1.47 | |
| S3-30NN | | | | | 2.94 | – |
| S3-00PS | | | | | 0.0 | Studs were welded |
| S3-00PN | | | | | | Without studs |
| S4-00NN | 4.5 | 135 | 9 | 30 | | – |

Table 1 Parameters of the specimens (Ozaki et al., 2004)

### 3.2. Test results

As the object of our study is pure in-plane behaviour of the SCS, the most relevant results are related to the specimens S2-00NN, S3-00NN, S4-00NN. Figure 5 shows the comparison of the responses of the above named panels.

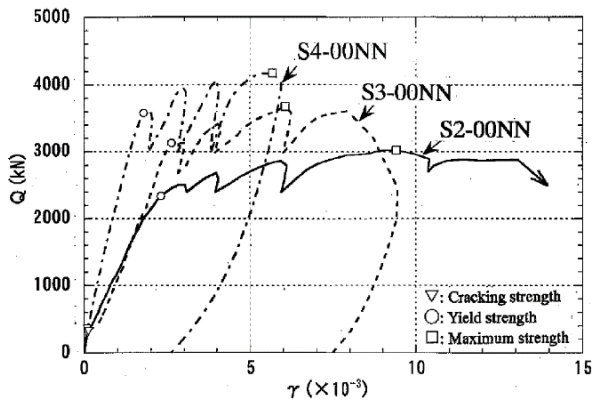


Figure 5 Response of relevant specimens (Ozaki et al., 2004)

It is obvious that as the thickness of the steel plates increases, the ultimate shear resistance increases and the ductility decreases. The interesting fact is that the addition of the partitioning web caused the increase of the ductility of the panel S3-00PS and S3-00PN while the ultimate resistance remained the same as that of the panel S3-00NN with the same thickness of the steel plates.

A summary of the results which are used for calibration of the numerical nonlinear model is presented in the Table 2.

| Specimen | Steel | | Concrete | Elastic shear modulus | Post-cracking shear modulus | Cracking strength | | Yield strength | | Maximum strength | |
|---|---|---|---|---|---|---|---|---|---|---|---|
| | Yield stress, Young's modulus (MPa) | $A_w \times A_p$ ($cm^2$) | Compressive strength, tangential stiffness (MPa) | $G_c$ ($\times 10^3$ MPa) | $G_y$ ($\times 10^3$ MPa) | $Q_c$ (kN) | $\gamma_c$ ($\times 10^{-3}$) | $Q_y$ (kN) | $\gamma_y$ ($\times 10^{-3}$) | $Q_u$ (kN) | $\gamma_u$ ($\times 10^{-3}$) |
| S2-00NN | 340 ($1.97\times10^5$) | 53.5 (17.1) | 42.2 ($2.72 \times 10^4$) | 12.4 | 4.16 | 293 | 0.115 | 2290 (−2110) | 2.50 (−1.99) | 2960 (−2780) | 9.41 (−6.12) |
| S2-15NN | | | 41.6 ($2.77 \times 10^4$) | 13.2 | 4.14 | 433 | 0.133 | 2330 (−2290) | 2.71 (−2.21) | 3110 (−2930) | 10.00 (−6.02) |
| S2-30NN | | | 42.0 ($2.79 \times 10^4$) | 16.4 | 3.69 | 542 | 0.168 | 2490 (−2570) | 3.01 (−2.41) | 3110 (−3200) | 10.48 (−6.03) |
| S3-00NN | 351 ($1.99 \times 10^5$) | 75.4 (16.9) | 41.9 ($2.71 \times 10^4$) | 12.9 | 4.88 | 311 | 0.134 | 3070 (−3070) | 3.01 (−2.00) | 3610 (−3430) | 6.05 (−6.03) |
| S3-15NN | | | 41.6 ($2.67 \times 10^4$) | 13.1 | 4.29 | 384 | 0.141 | 3130 (−3120) | 2.99 (−3.01) | 3760 (−3330) | 7.99 (−6.01) |
| S3-30NN | | | 40.1 ($2.70 \times 10^4$) | 11.9 | 4.67 | 385 | 0.186 | 3170 (−3080) | 2.80 (−2.96) | 3730 (−3550) | 5.57 (−5.63) |
| S3-00PS | | 75.4 (25.4) | 41.9 ($2.71 \times 10^4$) | 13.1 | 5.81 | 350 | 0.141 | 2680 (−2640) | 1.93 (−1.97) | 3580 (−3220) | 10.87 (−5.98) |
| S3-00PN | | | 39.9 ($2.72 \times 10^4$) | 16.4 | 4.92 | 271 | 0.113 | 2350 (−2390) | 2.01 (−2.03) | 3510 (−3060) | 17.00 (−6.02) |
| S4-00NN | 346 ($2.07 \times 10^5$) | 104.9 (16.7) | 42.8 ($2.76 \times 10^4$) | 16.4 | 8.22 | 349 | 0.103 | 3510 (−3560) | 2.01 (−2.00) | 4100 (−3790) | 5.67 (−4.00) |

Table 2 Test results (Ozaki et al., 2004)

## 4. NONLINEAR ANALYSIS

### 4.1. General

A nonlinear analysis was realized through the software ATENA from the company Červenka Consulting s.r.o.

The aim was to simplify the model as much as possible but still keep the parameters of the panels from experiment. The concrete core was modelled as a volume with in-plane dimensions 1200x1200 mm and a thickness 200 mm – 2*$t_s$. The steel plates were modelled as square shells fully tied to the concrete element. As result, the model considers full composite action.

### 4.2. Materials

The most basic material parameters of steel (yield stress, Young´s modulus) and concrete (compressive strength, tangential stiffness) are noted in the Table 2. The Poisson's constant was considered as 0,3 for steel and 0,2 for concrete. The rest parameters, especially for concrete, were chosen to correspond to C40/50 strength class of concrete accoring to Eurocode 2.

### 4.3. Boundary conditions

Since the model is about to be calibrated with the test results, boundary conditions should correspond to the test setup as well. Uniform in-plane forces were applied to the panels using the shear bolts test facility (see Figure 6). The facility was comprised of a self-reacting frame containing eight hydraulic jacks.

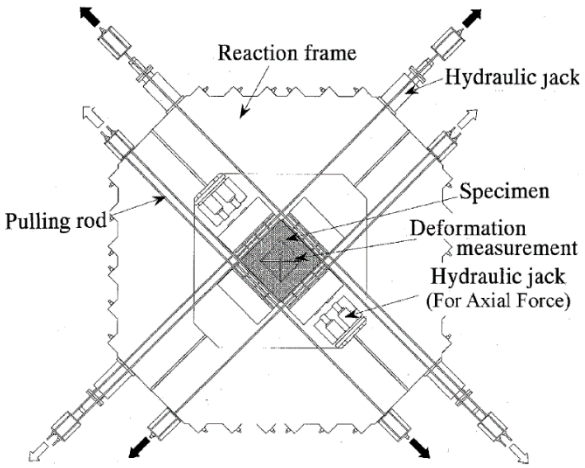


Figure 6 Test setup (Ozaki et al., 2004)

The model was loaded by forces, which were applied on edge surfaces of the concrete volume. The direction of the forces corresponds to pure shear.

Supports of the model should satisfy these conditions. It has to support the model enough to avoid instability, but has to be released enough to provide extention of the model. According to that, the edge surfaces of the model were supported by springs with a stiffness of 1000 MPa in transverse direction of the edge. The centroid of the concrete core model as supported in all directions.

Boundary condition are shown in Figure 7.

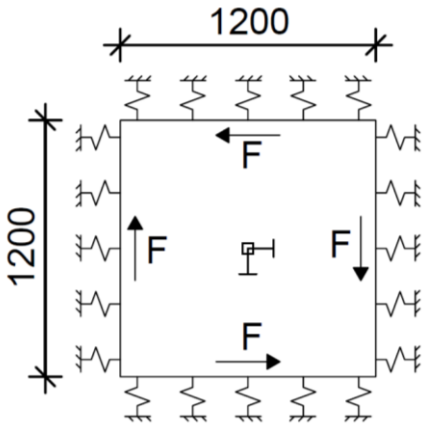


Figure 7 Boundary condition

### 4.4. Results

A calculation has been carried on five models with the different reinforcement ratio 2.3%, 3.2%, 4.5%, 10%, and 13%. Every model has had the same hexahedra type mesh with 10 x 10 number of cells longitudinally and one cell transversely. The shear-force load-deflection diagrams of the models are stated below.

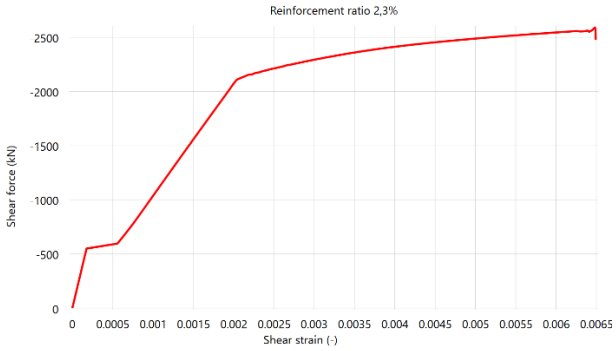


Figure 8 Shear-force load-deflection diagram of the model with the reinforcement ratio 2.3%

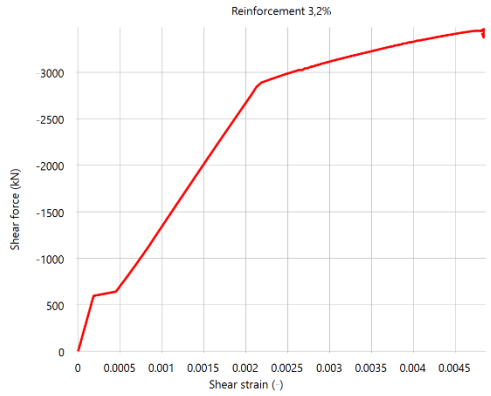


Figure 9 Shear-force load-deflection diagram of the model with the reinforcement ratio 3.2%

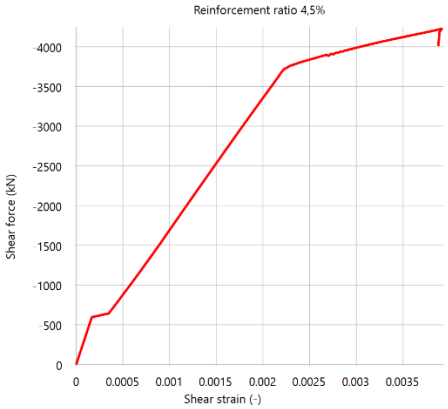


Figure 10 Shear-force load-deflection diagram of the model with the reinforcement ratio 4.5%

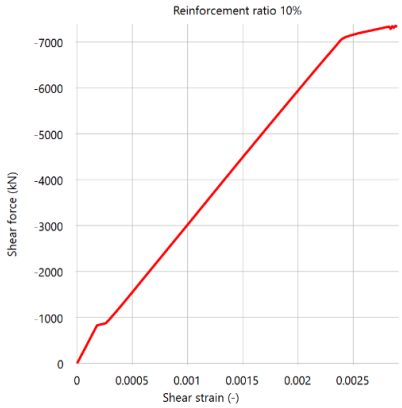


Figure 11 Shear-force load-deflection diagram of the model with the reinforcement ratio 10%

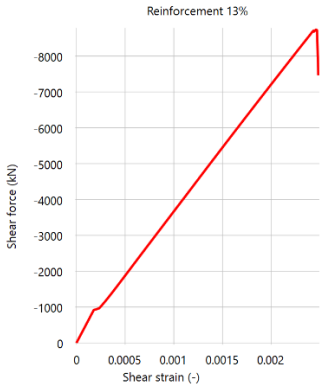


Figure 12 Shear-force load-deflection diagram of the model with the reinforcement ratio 13%

All the calculations ended, when concrete cracking occurred, while the yield point of steel has been already reached.

## 5. CONCLUSIONS

The results on the models with the reinforced ratio 2.3%, 3.2%, and 4.5%. correlate well to Japanese test results. It is good to note that the ductility of the nonlinear models is a bit lower compared to the specimens, but the plastic part of the diagram tends to be shorter as the reinforcement ratio rises, which is in accordance to the experiments.

The other two models represent the extrapolation. These two indicate that the possibility of failure mode change is real. Furthermore, the brittle failure is about to occur when the reinforcement ratio reaches 13%.

The limit that is given by the code – 5 % reinforcement ratio – is definitely reasonable. However, higher reinforcement may be necessary in some cases. The undesirable mode of failure of heavily reinforced SCS structures provides a challenge to make an improvement, which would provide better ductility. Maybe, adding a partitioning web might be the solution. Figure 13 shows the influence of a partitioning web.

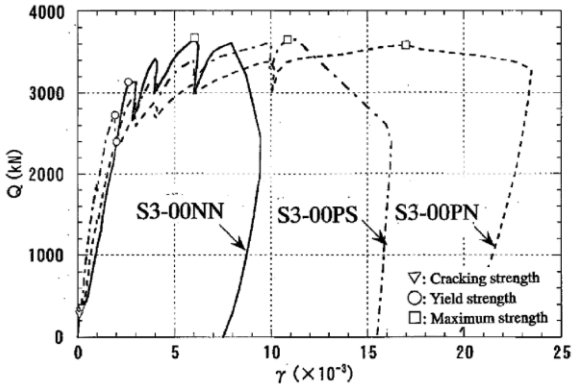


Figure 13 Comparison of specimen S3-00NN (without partitioning web), S3-00PS (partitioning web with stud bolts), S3-00PN (partitioning web without stud bolts) (Ozaki et al., 2004)

**ACKNOWLEDGEMENTS**

The research activities were supported by the Technology Agency of the Czech Republic under the THETA program, project no. TK01030116 “Conceptual design of safety-important components of helium-cooled fast demonstration reactor ALLEGRO”, and by the Czech Technical University in Prague under student project no. SGS22/091/OHK1/2T/11 “Experimental and numerical analysis of concrete and fibre-reinforced concrete for special applications”.

# References

ANSI/AISC N690-18 (2018), Specification for Safety-Related Steel Structures for Nuclear Facilities, American Institute of Steel Construction.

Varma, A.H., Zhang, K., Chi, H., Booth, P.N. and Baker, T. (2011), “In-Plane Shear Behavior of SC Walls: Theory vs. Experiment,” Transactions of the Internal Association for Structural Mechanics in Reactor Technology Conference, SMiRT-21, Div. X Paper 761, New Delhi, India, IASMIRT, North Carolina State University, Raleigh, NC.

Ozaki, M., Akita, S., Oosuga, H., Nakayama, T. and Adachi, N. (2004), “Study on Steel Plate Reinforced Concrete Panels Subjected to Cyclic In-Plane Shear,” Nuclear Engineering and Design, Vol. 228, pp. 225−244.

Sasaki, N., Akiyama, H., Narikawa, M., Hara, K., Takeuchi, M., Usami, S., 1995. Study on a Concrete Filled Steel Structure for Nuclear Power Plants (Part 2) Compressive Loading Tests on Wall Members. Transactions of the 13th International Conference on Structural Mechanics in Reactor Technology, vol. H. Porto Alegre, Brazil, pp. 21–26.

EN 1992-1-1: Eurocode 2: Design of concrete structures - Part 1-1: General rules and rules for buildings